HHS Public Access

Author manuscript

JACC Clin Electrophysiol. Author manuscript; available in PMC 2022 July 01.

Published in final edited form as:

JACC Clin Electrophysiol. 2021 July ; 7(7): 923–932. doi:10.1016/j.jacep.2020.12.005.

Epiphenomenal Re-Entry and Spurious Focal Activation Detection by Atrial Fibrillation Mapping Algorithms

Majd E. Hemam, MD[a,b], **Amish S. Dave, MD, PHD**[a], **Moisés Rodríguez-Mañero, MD**[c], **Miguel Valderrábano, MD**[a]

[a]Division of Cardiac Electrophysiology, Houston Methodist DeBakey Heart and Vascular Center, Houston, Texas, USA

[b]Department of Medicine, Rutgers New Jersey Medical School, Newark, New Jersey, USA

[c]Complexo Hospitalario Universitario de Santiago de Compostela (CHUS), Santiago de Compostela, Spain

Abstract

OBJECTIVES—The purpose of this study was to validate the ability of mapping algorithms to detect rotational activations (RoA) and focal activations (FoA) during fibrillatory conduction (FC) and atrial fibrillation (AF) and understand their mechanistic relevance.

BACKGROUND—Mapping algorithms have been proposed to detect RoA and FoA to guide AF ablation.

METHODS—Rapid left atrial pacing created FC—fibrillatory electrograms—with and without AF induction in dogs (n = 17). Activation maps were constructed using Topera (Abbott, St. Paul, Minnesota) or CARTOFINDER (Biosense Webster, Irvine, California) algorithms. Mapping strategies included: panoramic noncontact mapping with a basket catheter (CARTOFINDER n = 6, Topera n = 5); and sequential contact mapping using 8-spline OctaRay catheter (Biosense Webster) (n = 6). Offline frequency and spectral analysis were also performed. Algorithm-detected RoA was manually verified.

RESULTS—The right atrium (RA) consistently exhibited fibrillatory signals during FC. FC with and without AF had similar left-to-right frequency gradients. Basket maps were either uninterpretable (847 of 990 Topera, 132 of 148 Cartofinder) or had unverifiable RoA. OctaRay contact mapping showed 4% RoA (n = 30 of 679) and 63% FoA (n = 429 of 679). Verified RoA clustered at consistent sites, was more common in the RA than left atrium (odds ratio: 3.5), and colocalized with sites of frequency breakdown in the crista terminalis and RA appendage. During pacing, spurious FoA sites were identified around the atria, but not at the actual pacing sites.

ADDRESS FOR CORRESPONDENCE: Dr. Miguel Valderrábano, Division of Cardiac Electrophysiology, Department of Cardiology, Houston Methodist Hospital, 6550 Fannin Street, Suite 1901, Houston, Texas 77030, USA. mvalderrabano@houstonmethodist.org.

APPENDIX For an expanded Methods section as well as supplemental tables and figures, please see the online version of this paper.

The authors attest they are in compliance with human studies committees and animal welfare regulations of the authors' institutions and Food and Drug Administration guidelines, including patient consent where appropriate. For more information, visit the Author Center.

RoA and FoA site distribution was similar during pacing with and without induction, and during induced AF.

CONCLUSIONS—Mapping algorithms were unable to detect pacing sites as true drivers of FC, and detected epiphenomenal RoA and FoA sites unrelated to AF induction or maintenance. Algorithm-detected RoA and FoA did not identify true AF drivers.

Keywords

3D; atrial fibrillation; CARTOFINDER; focal activation; frequency; mapping; repetitive patterns; rotational activation; rotors; spectral analysis

Despite decades of research, the fundamental mechanisms of atrial fibrillation (AF) are unclear. Re-entry in AF has been postulated for over a century (1), and has gained support from frequency analysis of optical mapping studies (2,3). Yet, definite proof has been elusive, because most mapped re-entrant episodes were too short (1 to 2 rotations) (4) to be considered stable AF drivers. Focal, repetitive activations have also been proposed for decades to drive AF (5,6), and also have some experimental support (7,8). Thus, multiple mapping systems have been developed to identify sites with focal activations (FoA) and/or rotational activations (RoA) during AF. These sites have been assumed to be mechanistically relevant to the maintenance of AF and consequently suggested as ablation targets to eliminate AF (9). Because local propagation patterns are influenced by myofiber architecture, areas of unidirectional block and apparent re-entry may arise during AF; such apparent spurious re-entry may not bear mechanistic relevance, and yet may be identified as relevant by mapping system algorithms. Similarly, apparent focal propagation patterns may be identified when a restricted area is mapped away from a remote source of propagation.

Fibrillatory conduction (FC), characterized by intermittent unidirectional block, arises in areas of anatomical heterogeneity and generates fibrillatory electrograms during rapid pacing in the absence of true, self-sustained AF, as shown by Berenfeld et al. (10) in isolated sheep atria. This phenomenon permits testing of the performance of mapping systems in a “negative control” condition where no true, self-sustained AF exists, and any RoA or FoA detected away from the pacing site(s) is, by definition, epiphenomenal. Systems to map propagation patterns in AF, like Topera (Abbott, St. Paul, Minnesota) (11) or CARTOFINDER (Biosense Webster, Irvine, California) (12), have been developed but have never been studied in such an experimental model of FC.

The goal of this study was to explore the mechanistic relevance of RoA and FoA and to assess the ability of algorithms to detect such activity during in vivo canine models of pacing-induced FC and induced AF.

METHODS

STUDY DESIGN.

Healthy mongrel dogs (n = 17) were subjected to general anesthesia. Vascular access was obtained using the right femoral and internal jugular veins. A duodecapolar catheter was positioned so the 10 distal poles were in the coronary sinus (CS) and the 10 proximal poles

in the right atrium (RA). Two transseptal punctures were performed: one for a decapolar catheter inserted in the right superior pulmonary vein (RSPV), and the other for the mapping catheter (Figure 1). The protocol was approved by the Houston Methodist Research Institute Institutional Animal Care and Use Committee.

PACING PROTOCOL.

Bipolar pacing was performed using electrodes from RSPV, distal CS, or both simultaneously until FC was observed. Dual-site, dual-pacing cycle length facilitated induction of FC. Induced AF was defined as fibrillation sustained for at least 30 s after cessation of pacing. Maps and analyses of AF were conducted during self-sustained AF without pacing. Discrimination of pacing-induced FC versus underlying AF while pacing was performed by the absence of self-sustained AF after pacing. Electrograms were collected with a Bard recording system (Labsystem PRO, Boston Scientific, Marlborough, Massachusetts) at 4 kHz, and were exported for offline analysis. Panoramic basket catheter mapping (n = 5 with Topera, n = 6 with CARTOFINDER) or sequential OctaRay (CARTOFINDER, n = 6) was performed, identifying RoA or FoA with their respective algorithms.

Full details of frequency analysis, mapping protocols, elimination of pacing artifact, and statistical analyses are available in the Supplemental Appendix (Supplemental Figures 1, 2, and 3).

RESULTS

FREQUENCY ANALYSIS DURING FIBRILLATORY CONDUCTION AND CORRELATION WITH AF.

In all experiments, fibrillatory signals were observed in the RA during pacing despite 1:1 propagation in the left atrium (LA) and without induction of AF. Offline frequency analysis of pacing-induced AF episodes (n = 9) and fibrillatory electrograms during pacing-induced FC (n = 10) were analyzed from experiments in 6 dogs. Fibrillatory signals without AF induction were associated with a decreased regularity index (RI) (increased frequency variability) in the RA compared with the LA (41 ± 14%, 68 ± 27%, and 85 ± 17% for RA, CS, and RSPV, respectively; $p < 0.001$) (Figures 2D and 3). Spatial distribution of dominant frequency (DF) regularity during pacing with FC with and without AF induction were similar (Figure 2D). Left-to-right frequency gradient was also observed during induced AF (7.8 ± 0.6, 7.4 ± 0.8, and 7.0 ± 0.7 Hz for RSPV, CS, and RA, respectively; $p = 0.006$) (Figure 2E). An essential component of the model is FC, and generation of fibrillatory electrograms did not equal AF induction. In most instances, cessation of pacing led to sinus rhythm.

OctaRay mapping allowed us to perform frequency analysis in signals from the entire atrial anatomy. Figure 3 shows the spatial distribution of DF breakdown during FC created by RSPV pacing. The LA displays a uniform frequency distribution corresponding to the pacing frequency; yet, the RA shows a heterogeneous frequency map: the septum

maintains the pacing frequency, whereas the lateral RA wall shows a patchy distribution of frequencies. This location correlated with the induction of RoA (see the following text).

PANORAMIC BASKET CATHETER MAPPING (N = 5 WITH TOPERA, N = 6 WITH CARTOFINDER).

A total of 990 4-s Topera movies and 148 CARTOFINDER basket maps were analyzed. The vast majority of these showed complex activation patterns of meandering wavelets. Basket mapping-detected RoA had difficult anatomical interpretations and are described in Supplemental Figures 4, 5, and 6.

OctaRay GROUP (N = 6).

A total of 679 movies of 30-s duration during sequential mapping in the RA and LA (479 during pacing with FC, and 200 during induced AF) were constructed. Of these, 4.4% (n = 30 of 679) showed RoA (average rotations = 8.9 ± 6.7) whereas 63% (n = 429 of 679) showed FoA. The enhanced tissue contact and accurate electrode localization allowed anatomical correlations.

1. Focal activity
    a. During FC: 60% of the maps (n = 285 of 479) recorded during FC showed FoA, which appeared to be evenly distributed among the atrial sites (Supplemental Table 1) Despite pacing from left atrial sites only, FoA was commonly detected in the RA by the algorithm.
        i. During pacing from the RSPV: the system was able to detect the pacing site as an FoA in only 36% of the maps recorded in the RPV region (n = 5 of 14). The FoA detection rate was falsely high in other LA regions like the left atrial appendage (LAA) (55%; n = 6 of 11 of the LAA maps) and the floor (80%; n = 8 of 10 of the floor maps), all while pacing from the RSPV. In the RA, 44% (n = 35 of 79) of the maps showed FoA, with the highest rate of FoA detection in the septum (57%; n = 8 of 14 of the septal maps) and crista terminalis (CT) (57%; n = 16 of 28 of the CT maps) (Supplemental Table 1, Figure 4A).
        ii. Pacing from the CS: FoA was detected in the LPV (91%; n = 10 of 11 of the LPV maps), floor (86%; n = 12 of 14 of the floor maps), and LAA (73%; n = 8 of 11 of the LAA maps) among other regions. However, other LA regions were also labeled as having FoA despite the fact that we were pacing from a known location in the CS (Supplemental Table 1, Central Illustration, Figure 4B). In the RA, 60% (n = 40 of 67) of the maps showed FoA, with the highest rate in the septum 80% (n = 8 of 10 of the septal maps).
        iii. During dual-site pacing (RSPV and CS): LA maps showed FoA detection rate of 20% (n = 3 of 15) in the RPV, 75%

(n = 6 of 8) in the LPV, and 75% (n = 12 of 16) in the LAA (Supplemental Table 1). In the RA, 57% (n = 31 of 54) of the maps showed FoA. The highest rate of FoA detection in the RA was in the septum (78%; n = 7 of 9). (Figure 5, Supplemental Table 1). Figure 5 shows DF maps during dual-site, dual cycle length pacing. In this case shown, neither pacing cycle length was sufficiently short to induce FC by itself (180 ms from CS and 200 ms from RSPV), but combined they show occasional fibrillatory electrograms. The DF maps show how areas surrounding pacing sites have DFs matching their cycle length (5 Hz for 200 ms in RSPV, 5.6 Hz for 180 ms from distal CS). The bulk of the anterior LA and RA have a DF of 5.6, whereas the area around the RSPV and SVC has a DF of 5 Hz. The posterior wall has a patchy DF distribution. RI maps for each frequency illustrate the regional frequency dominance. Of note, the algorithm failed to detect FoA in either pacing site and falsely detected spurious FoA in the posterior LA wall and elsewhere.

b. During AF: 72% of the maps (n = 144 of 200) recorded during AF showed FoA. A detailed analysis showed no major differences in FoA detection rates between the LA (69%; n = 72 of 105) and RA (76%; n = 72 of 95) or among the atrial sites (Supplemental Table 1).

2. Re-entry

a. During FC: RoA was detected in 4.2% of the maps (n = 20 of 479) recorded during FC. RoA was more likely to be found in the RA (n = 14 of 200) than the LA (n = 6 of 279) (odds ratio [OR]: 3.4; p = 0.01). RoA during FC was significantly more likely to occur during distal CS pacing (7.3%; n = 11 of 150) than during RSPV pacing (1.1%; n = 2 of 177) (OR: 7; p = 0.008). Of the RoA during FC, 50% (n = 10 of 20) were in the right atrial appendage (RAA) and CT alone. The other 50% were evenly distributed over other RA and LA sites. The average number of rotations in the RA was 7.8 ± 6 (4.9 ± 1.1 CT, 8 RAA, 17.5 ± 10.5 septum, 9.5 ± 1.5 RA-SVC junction) and in the LA 10 ± 9.1 (3.5 ± 0.5 floor, 5 LAA, 9.5 ± 3.5 posterior wall, 29 roof). The location with highest incidence of RoA during FC (number of maps with RoA divided by the total number of maps from that region) was the CT (11.3%; n = 8 of 71 maps from CT) followed by the RAA (9.1%; n = 2 of 22 maps from the RAA). In fact, FC during CS pacing showed RoA in 1 of every 5 maps (n = 5 of 25) recorded in the CT region (Table 1, Supplemental Table 2).

b. During AF: RoA was detected in 5% of the maps(n = 10 of 200) recorded during AF. RoA did not follow a random spatial distribution. RoA was more likely to be found in the RA (n = 8 of 95) than the LA

(n = 2 of 105) (OR: 4.7; p = 0.049). During AF, 60% (n = 6 of 10) of the RoA detected occurred in the CT and RAA. The average number of rotations in the RA was 9.5 ± 5.9 (6 ± 0.8 in CT, 11 ± 6.7 in RAA, 6 in septum, 19 in RA-SVC junction) and in the LA was 11 ± 4 (7 in the floor, 15 in the posterior wall). The locations with highest incidence of RoA during AF was in the RAA (15%; n = 3 of 20) followed by the CT (9.7%; n = 3 of 31) (see Supplemental Table 2, Supplemental Figure 3).

For both FC and AF, the locations of re-entry matched the locations of frequency breakdown shown in the maps (compare Figure 3B with Supplemental Figure 3).

DISCUSSION

The main findings of this study were: 1) fibrillatory signals arose in the RA during rapid in vivo LA pacing despite 1:1 propagation in the LA and without induction of AF (Figure 2A); 2) spatial distribution of DF and its regularity index during pacing with FC with and without AF induction and during ongoing AF are similar (Figures 2 and 3); 3) panoramic mapping with the basket catheter most commonly led to uninterpretable data; 4) RoA during FC or AF was rare, and occurred more commonly in RA than LA (OR: 3.5) and during pacing from distal CS than from RSPV (OR: Majority of RoA detected in the RA (Central Illustration), and these locations match the locations of DF breakdown during pacing with FC (Figure 3B); and 6) FoA detection algorithms were unable to localize true focal sources during pacing.

SPECTRAL CHARACTERISTICS OF PACING-INDUCED FIBRILLATORY CONDUCTION AND INDUCED AF.

Consistent with other studies (13,14), we found a left-to-right frequency gradient during pacing-induced AF, which has been attributed to the left-to-right inward rectifier potassium current gradients (15,16) and was found to occur in both pacing-induced and spontaneous human AF (17). We also confirm gradients of organization of fibrillation (as shown by RI gradients) between the LA and RA. We expand these findings by demonstrating that similar spatial gradients of DF and organization occur during pacing with FC both *with and without* AF induction (Figure 2D). The latter observation both points toward a site-specific tissue property as the basis for this variability in organization and shows that gradients in DF and RI occur in the absence of AF inducibility and cannot be considered mechanistically inherent to AF.

FIBRILLATORY ELECTROGRAMS IN THE ABSENCE OF INDUCED AF.

Despite regular 1:1 propagation and regular signals in the LA, the RA showed fibrillatory electrograms (see RA signals during pacing in Figure 2A and point 3 time and frequency domains in Figure 3). This disruptive conduction, however, did not necessarily induce AF, as evidenced by the disappearance of fibrillatory electrograms and restoration of sinus rhythm post-pacing (Figures 2A, Central Illustration). The fact that fibrillatory signals exist in the absence of sustained AF is clinically relevant. Fibrillatory electrogram complexity (18) and frequency content (19) have been used to attribute mechanistic relevance to different sites in atrial fibrillation as targets for ablation therapy (20). We show that the complexity and

spectral characteristics of fibrillatory electrograms in the RA occur in the absence of AF induction (Figure 2D). Although the phenomenon of FC in the RA has been described by Berenfeld et al. (10) in ex vivo tissues, the current study shows that the mere presence of this FC is not sufficient for self-regeneration and sustainment of fibrillation.

Additionally, we show that dual-site, dual-cycle length pacing can induce complex propagation patterns with fibrillatory electrograms that, in the absence of AF induction, can lead to complex frequency distribution maps.

RoA DURING PACING AND AF.

The CARTOFINDER algorithm detected RoA in 4.2% (n = 20 of 479) of the OctaRay maps during rapid pacing with FC. The presence of such RoA—confirmed manually in all cases—did not correlate with the induction of AF. Such apparent RoA arose as propagating wave fronts from the pacing site encountered unidirectional block (anatomically determined by local heterogeneities) that led to a local rotation around the site of block. Consistent with Berenfeld et al. (10) and our previous observations in fibrillating ventricles (21), abrupt fiber orientation changes can lead to the formation of local re-entrant propagation, and as in those studies, such RoA occurs at the very sites (Central Illustration) of frequency breakdown (Figure 3B). The fact that this RoA exists in the absence of sustained AF proves that algorithm-detected RoA is not sufficient to qualify an RoA as an independent driver of AF—the only true “driver” during LA pacing-induced FC is the pacing stimulus—and questions the mechanistic relevance of indiscriminately using ablation techniques targeting algorithm-detected RoA.

We found greater incidence of RoA in the RA during CS pacing than during RSPV pacing. Although the specific mechanism for this finding is speculative, the closer proximity of the RSPV to the RA may limit the number of anatomical complexities propagation waves encounter as they reach the RA. The fact that the incidence of RoA in the RA could be modulated by the site of LA pacing—and yet be clustered in the same locations—illustrates the interplay between dynamic and fixed factors. Fixed heterogeneities in the RAA-crista terminalis connection are potential sites of anisotropic unidirectional conduction block and induction of re-entry (22).

The clinical relevance of our findings is that we show that such re-entry is entirely a passive phenomenon during pacing, and although mapping algorithms can detect it, such RoA cannot be conceived as a driver of self-sustained propagations, let alone ablation targets.

The incidence of RoA was low. It is possible that factors not tested here—such as shortening action potential duration or conduction velocity slowing—may be present in clinical AF and promote RoA to greater incidences than what was found in our study.

FOCAL ACTIVITY DURING PACING AND AF.

We mapped FC during a known-site pacing to test the ability of the mapping algorithms to identify FoA in a controlled fashion. FoA detection by the mapping system was suboptimal, both failing to identify the pacing site (Figure 4), and erroneously identifying focal sources in areas remote from the pacing sites(s), including the RA, despite pacing from known LA

sites only. The algorithm identifies the earliest QS pattern within 50 ms of a single OctaRay recording. The QS criterion proved to be prone to errors (limited specificity and sensitivity) considering the limited spatial sampling. Among the FoA identified in the RA during pacing from LA sites, the RA septum had the highest FoA detection rate (Supplemental Table 1), suggesting that passive activation from the LA might have been labeled as a focal source in the RA. Thus, the relatively high FoA detection rate in this model represents a failure of the algorithm.

THE SHORTCOMINGS OF PANORAMIC MAPPING.

Panoramic mapping using the basket catheter frequently showed uninterpretable results. The anatomical correlation of Topera maps depends on arbitrary assessments of electrode location. Using Cartofinder, for any given recording, multiple electrograms were discarded due to insufficient proximity to the atrial wall—an unavoidable problem that Topera masks. Although we cannot disprove the reported clinical utility (23,24) or value of other catheter designs, we found the challenge of obtaining meaningful signals from a whole atrial chamber unsurmountable given the anatomical complexities.

STUDY LIMITATIONS.

FC and pacing-induced AF episodes in healthy, young canines were short and with low incidence of RoA, and they may be mechanistically distinct from clinical AF in humans. Future studies can focus on testing the algorithm in chronic AF models to better mimic persistent AF. Pacing artifacts could have affected our frequency analyses. Although we show that RoA can be epiphenomenal during FC, we cannot disprove that RoA may contribute to AF maintenance in clinical AF.

CONCLUSIONS

In the context of FC without AF induction, where any FoA sites other than the pacing site are spurious and any RoA is epiphenomenal, mapping algorithms failed to localize pacing sites as the true FoA origin, and instead identified spurious FoA sites and epiphenomenal RoA. Thus, phenomenological identification of FoA and RoA by current AF mapping algorithms may not be reliable for mechanistic inferences or for guiding AF ablation.

Supplementary Material

Refer to Web version on PubMed Central for supplementary material.

FUNDING SUPPORT AND AUTHOR DISCLOSURES

This study was supported by the Lois and Carl Davis Centennial Chair, the Charles Burnett III endowment, the Antonio Pacifico fellowship fund, and National Heart, Lung, and Blood Institute grant R01HL115003. Biosense-Webster donated catheters and lent processing workstations for this study. Dr. Valderrábano has received consulting and speaking honoraria from Biosense Webster and Boston Scientific. All other authors have reported that they have no relationships relevant to the contents of this paper to disclose.

ABBREVIAT IONS AND ACRONYMS

CS coronary sinus

DF	dominant frequency
FC	fibrillatory conduction
FoA	focal activations
RI	regularity index (of the dominant frequency)
RoA	rotational activations
RSPV	right superior pulmonary vein

REFERENCES

1. Mines GR. On dynamic equilibrium in the heart. J Physiol 1913;46:349–83. [PubMed: 16993210]
2. Mandapati R, Skanes A, Chen J, Berenfeld O, Jalife J. Stable microreentrant sources as a mechanism of atrial fibrillation in the isolated sheep heart. Circulation 2000;101:194–9. [PubMed: 10637208]
3. Skanes AC, Mandapati R, Berenfeld O, Davidenko JM, Jalife J. Spatiotemporal periodicity during atrial fibrillation in the isolated sheep heart. Circulation 1998;98:1236–48. [PubMed: 9743516]
4. Chen J, Mandapati R, Berenfeld O, Skanes AC, Gray RA, Jalife J. Dynamics of wavelets and their role in atrial fibrillation in the isolated sheep heart. Cardiovasc Res 2000;48:220–32. [PubMed: 11054469]
5. Prinzmetal M, Corday E, Brill IC, et al. Mechanism of the auricular arrhythmias. Circulation 1950;1:241–5. [PubMed: 15403029]
6. Scherf D, Terranova R. Mechanism of auricular flutter and fibrillation. Am J Physiol 1949;159: 137–42. [PubMed: 15391089]
7. Lee S, Sahadevan J, Khrestian CM, Cakulev I, Markowitz A, Waldo AL. Simultaneous biatrial high-density (510–512 electrSodes) epicardial mapping of persistent and long-standing persistent atrial fibrillation in patients: new insights into the mechanism of its maintenance. Circulation 2015;132:2108–17. [PubMed: 26499963]
8. de Groot N, van der Does L, Yaksh A, et al. Direct proof of endo-epicardial asynchrony of the atrial wall during atrial fibrillation in humans. Circ Arrhythm Electrophysiol 2016;9:e003648.
9. Calvo D, Rubin J, Perez D, Moris C. Ablation of rotor domains effectively modulates dynamics of human: long-standing persistent atrial fibrillation. Circ Arrhythm Electrophysiol 2017;10:e005740.
10. Berenfeld O, Zaitsev AV, Mironov SF, Pertsov AM, Jalife J. Frequency-dependent breakdown of wave propagation into fibrillatory conduction across the pectinate muscle network in the isolated sheep right atrium. Circ Res 2002;90: 1173–80. [PubMed: 12065320]
11. Narayan SM, Krummen DE, Enyeart MW, Rappel WJ. Computational mapping identifies localized mechanisms for ablation of atrial fibrillation. PLoS ONE 2012;7:e46034.
12. Daoud EG, Zeidan Z, Hummel JD, et al. Identification of repetitive activation patterns using novel computational analysis of multielectrode recordings during atrial fibrillation and flutter in humans. J Am Coll Cardiol EP 2017;3:207–16.
13. Lazar S, Dixit S, Marchlinski FE, Callans DJ, Gerstenfeld EP. Presence of left-to-right atrial frequency gradient in paroxysmal but not persistent atrial fibrillation in humans. Circulation 2004; 110:3181–6. [PubMed: 15533867]
14. Ulphani JS, Ng J, Aggarwal R, et al. Frequency gradients during two different forms of fibrillation in the canine atria. Heart Rhythm 2007;4:1315–23. [PubMed: 17905337]
15. Voigt N, Trausch A, Knaut M, et al. Left-toright atrial inward rectifier potassium current gradients in patients with paroxysmal versus chronic atrial fibrillation. Circ Arrhythm Electrophysiol 2010;3:472–80. [PubMed: 20657029]
16. Atienza F, Almendral J, Moreno J, et al. Activation of inward rectifier potassium channels accelerates atrial fibrillation in humans: evidence for a reentrant mechanism. Circulation 2006;114:2434–42. [PubMed: 17101853]

17. Calvo D, Atienza F, Jalife J, et al. High-rate pacing-induced atrial fibrillation effectively reveals properties of spontaneously occurring paroxysmal atrial fibrillation in humans. Europace 2012;14:1560–6. [PubMed: 22696516]

18. Nademanee K, McKenzie J, Kosar E, et al. A new approach for catheter ablation of atrial fibrillation: mapping of the electrophysiologic substrate. J Am Coll Cardiol 2004;43:2044–53. [PubMed: 15172410]

19. Sanders P, Berenfeld O, Hocini M, et al. Spectral analysis identifies sites of high-frequency activity maintaining atrial fibrillation in humans. Circulation 2005;112:789–97. [PubMed: 16061740]

20. Atienza F, Almendral J, Jalife J, et al. Real-time dominant frequency mapping and ablation of dominant frequency sites in atrial fibrillation with left-to-right frequency gradients predicts long-term maintenance of sinus rhythm. Heart Rhythm 2009;6:33–40. [PubMed: 19121797]

21. Valderrabano M, Chen PS, Lin SF. Spatial distribution of phase singularities in ventricular fibrillation. Circulation 2003;108:354–9. [PubMed: 12835210]

22. Spach MS, Miller WT 3rd, Dolber PC, Kootsey JM, Sommer JR, Mosher CE Jr. The functional role of structural complexities in the propagation of depolarization in the atrium of the dog. Cardiac conduction disturbances due to discontinuities of effective axial resistivity. Circ Res 1982;50:175–91. [PubMed: 7055853]

23. Verma A, Sarkozy A, Skanes A, et al. Characterization and significance of localized sources identified by a novel automated algorithm during mapping of human persistent atrial fibrillation. J Cardiovasc Electrophysiol 2018;29:1480–8. [PubMed: 30230079]

24. Narayan SM, Krummen DE, Shivkumar K, Clopton P, Rappel WJ, Miller JM. Treatment of atrial fibrillation by the ablation of localized sources: CONFIRM (Conventional Ablation for Atrial Fibrillation With or Without FocSal Impulse and Rotor Modulation) trial. J SSAm Coll Cardiol 2012;60:628–36.

PERSPECTIVES

COMPETENCY IN MEDICAL KNOWLEDGE:

Several mapping algorithms have been used to attribute mechanistic relevance to FoA and RoA during AF and to guide therapy. Our data questions the validity of current algorithms and the basis to ablate areas based on algorithm-detected RoA or FoA.

TRANSLATIONAL OUTLOOK:

The mechanisms of AF remain elusive. Without denying FoA or RoA as mechanisms, the detection of epiphenomenal re-entry and spurious focal sources during FC questions the algorithms approach. Algorithm refinement beyond phenomenological findings of RoA and FoA is needed.

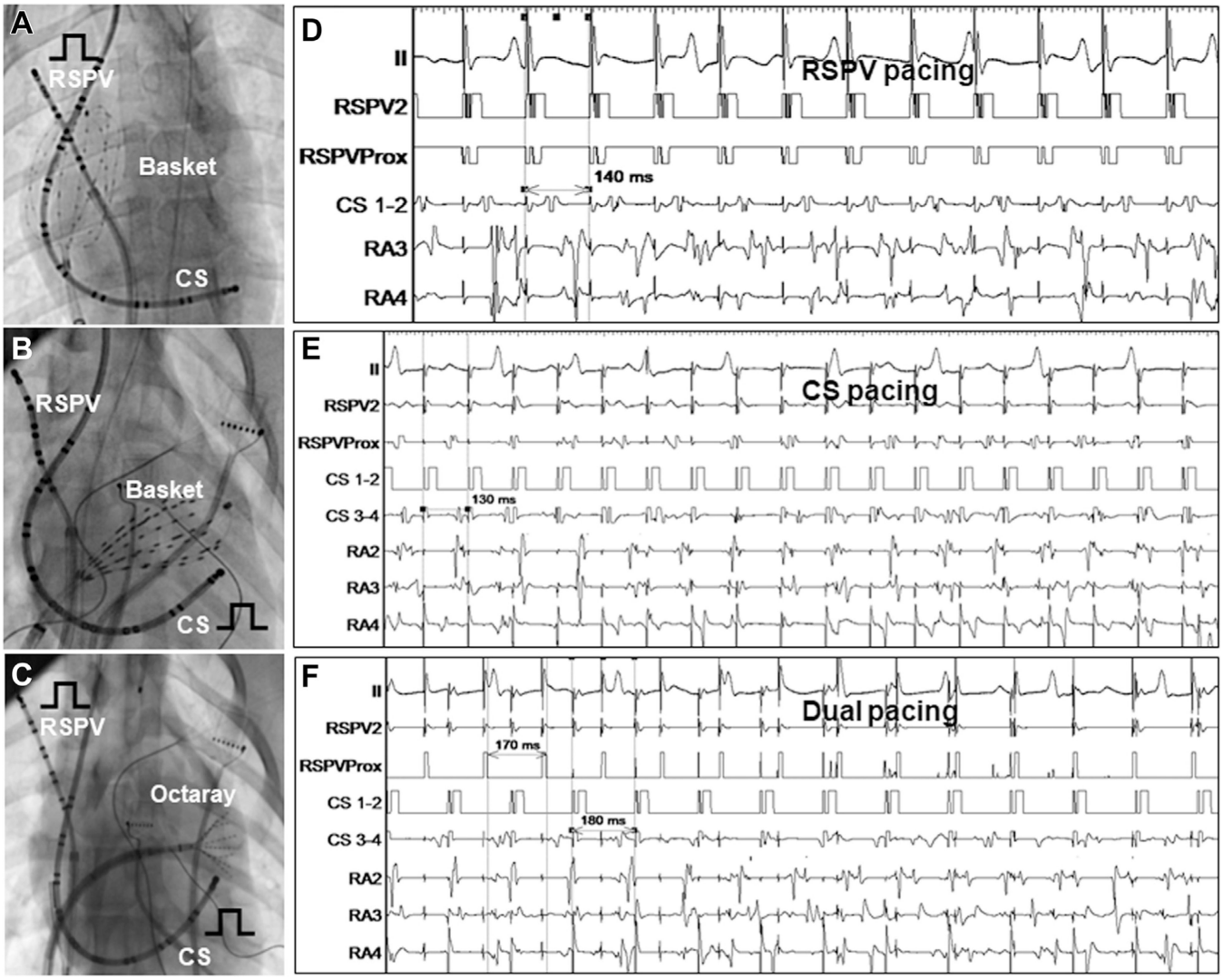

FIGURE 1. Experimental Setup

(**A to C**) Fluoroscopy of catheter arrangement. Basket catheter in the right atrium (RA) (**A**) and in the left atrium (LA) (**B**). (**C**) OctaRay catheter in the LA. (**D to F**) Examples of fibrillatory electrograms in the RA during rapid LA pacing from the right superior pulmonary vein (RSPV) (**D**), coronary sinus (CS) (**E**), or both (**F**).

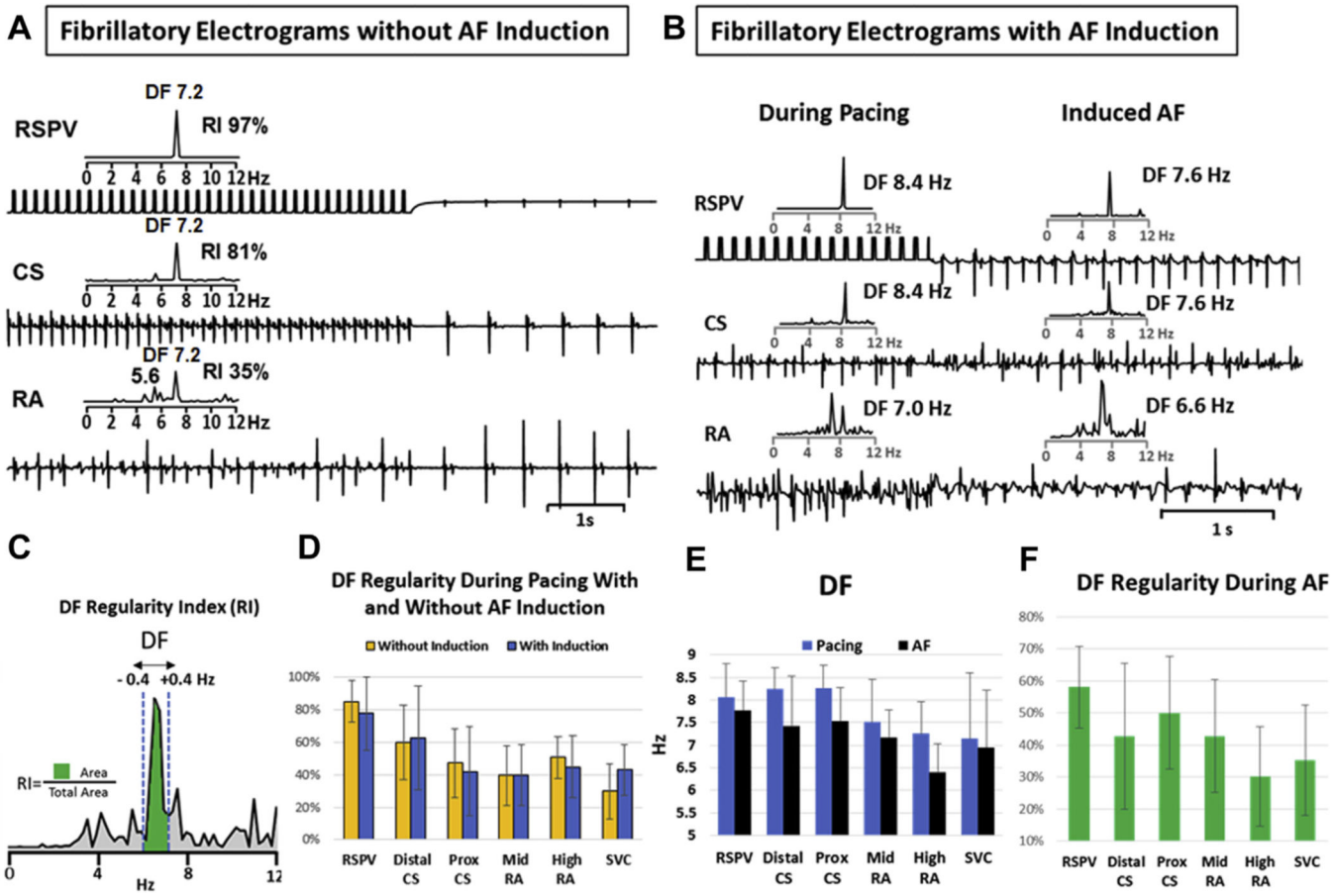

FIGURE 2. DF and its Regularity Index During Induced AF and Pacing With FC

(**A**) Fibrillatory electrograms during pacing from the RSPV at 140 ms (7.2 Hz) without AF induction. The phenomenon of FC is most apparent in the RA tracing. Note the decrease in RI of the DF in the frequency spectrum due to the less than 1-to-1 conduction underlying the FC. (**B**) Induced AF after pacing from the RSPV at 120 ms (8.4 Hz). (**C**) Schematic of RI frequency calculation. (**D**) DF regularity during pacing with and without AF induction: note the similar spatial distribution. (**E**) DF during pacing with FC and induced AF. Note the L-to-R frequency gradient between L and R atrial sites during AF. (**F**) DF regularity during AF. AF = atrial fibrillation; DF = dominant frequency; FC = fibrillatory conduction; L = left; R = right; RA = right atrium; RI = regularity index; RSPV = right superior pulmonary vein.

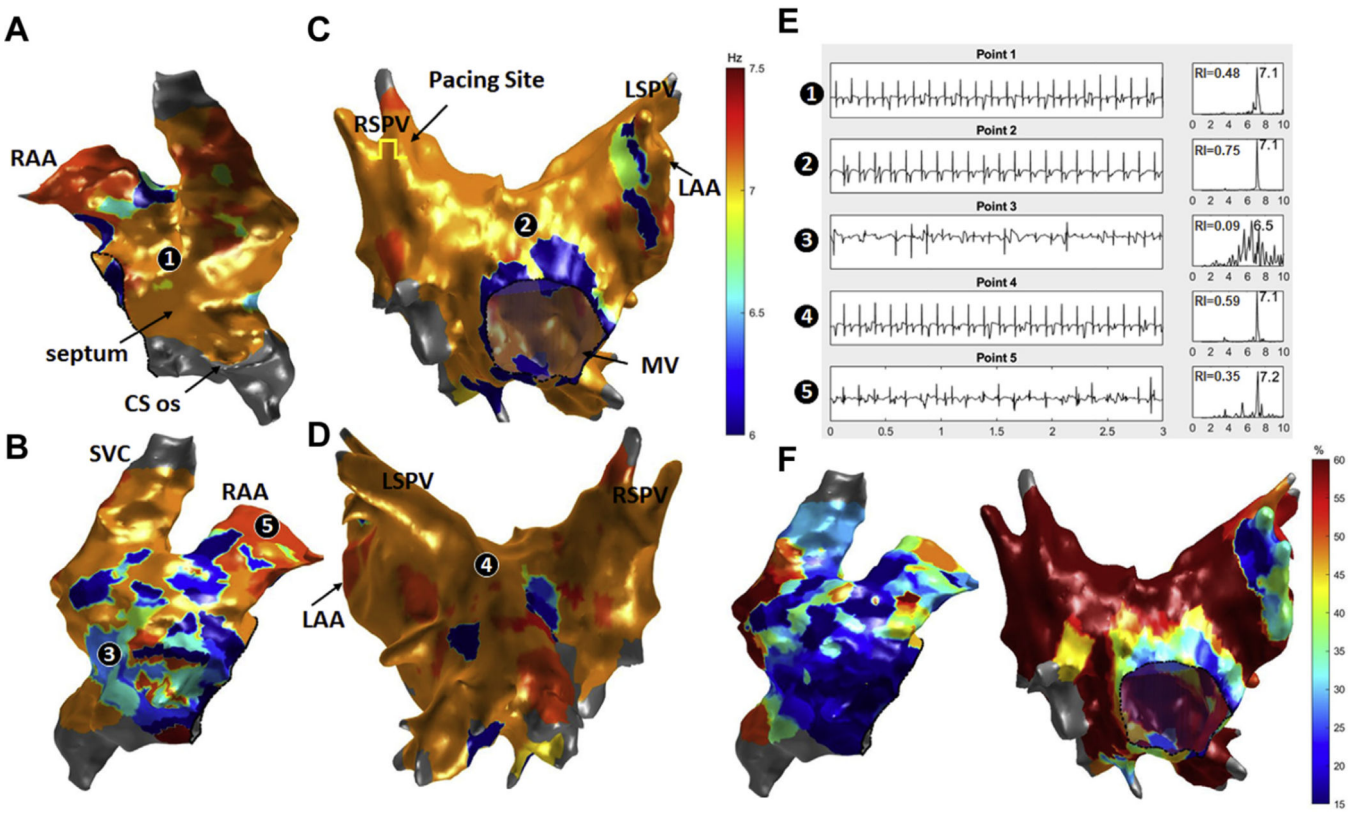

FIGURE 3. Dominant Frequency Maps During Pacing at 140 ms (7.1 Hz) From the RSPV With FC

Septal (**A**) and right lateral (**B**) view of the RA. AP (**C**) and PA (**D**) view of the LA. Note the frequency variation in the lateral wall of the RA (**B**) despite the 1-to-1 conduction in the LA (more uniform frequencies in **C** and **D**). (**E**) Time and frequency domains of the 5 points shown in **A** to **D**. Note the frequency breakdown and the less than 1-to-1 conduction in point 3 (corresponding to the crista terminalis in the RA). (**F**) DF regularity index maps showing the power ratio of the pacing frequency (7.1 Hz) in both atria. Note the increased frequency variability (less regularity) (**blue**) in the lateral wall of the RA due to the less than 1-to-1 conduction despite high regularity in the LA (**red**). Also note, spectral contamination with ventricular signals leads to decreased DF regularity around the mitral valve area. AP = anteroposterior; CS os = coronary sinus ostium; LAA = left atrial appendage; LSPV = left superior pulmonary vein; MV = mitral valve; PA = posteroanterior; RAA = right atrial appendage; SVC = superior vena cava; other abbreviations as in Figure 2.

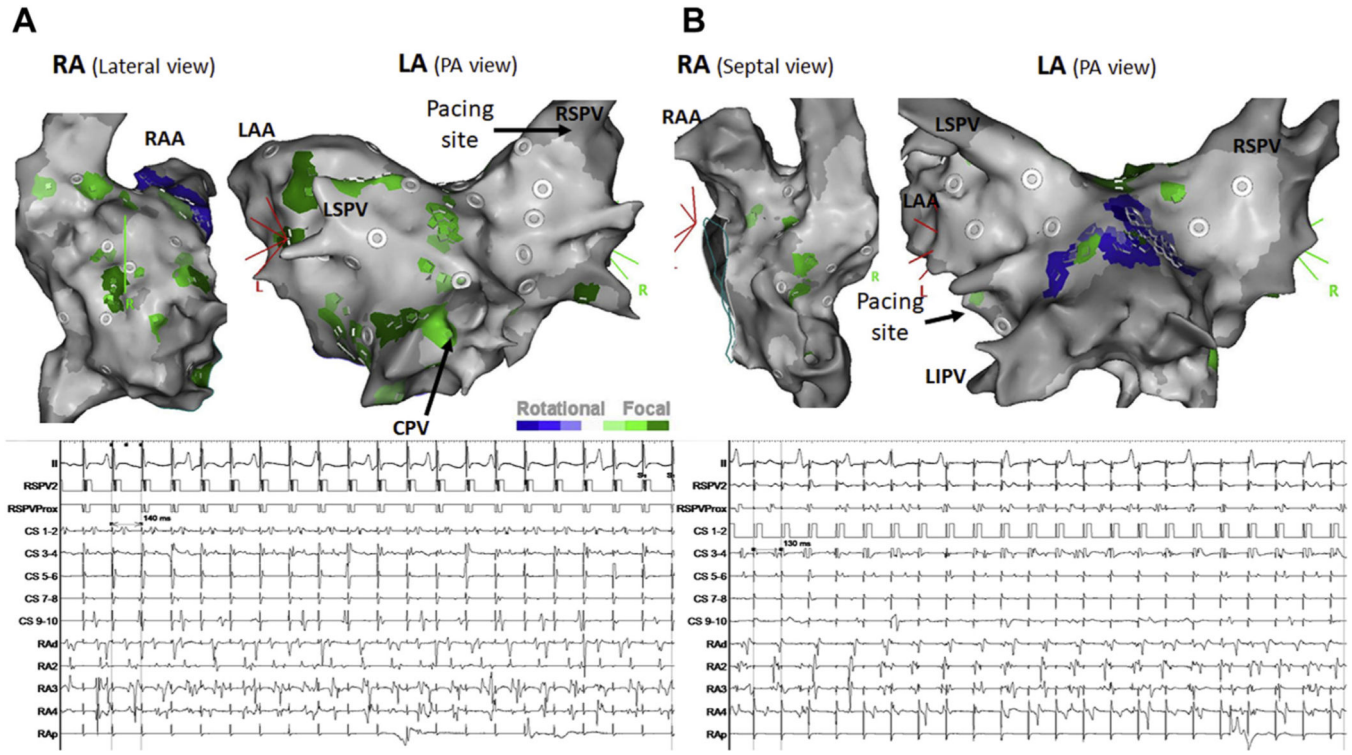

FIGURE 4. FoA Detection by the Cartofinder System

Lateral (**A**) and septal **(B**) view of the RA and PA view of the LA during pacing from the RSPV (**A**) and CS (**B**) showing FoA at distant sites. Note that the system fails to identify the pacing sites as an FoA. CPV = common pulmonary vein; FoA = focal activations; LIPV = left inferior pulmonary vein; other abbreviations as in Figures 1 to 3.

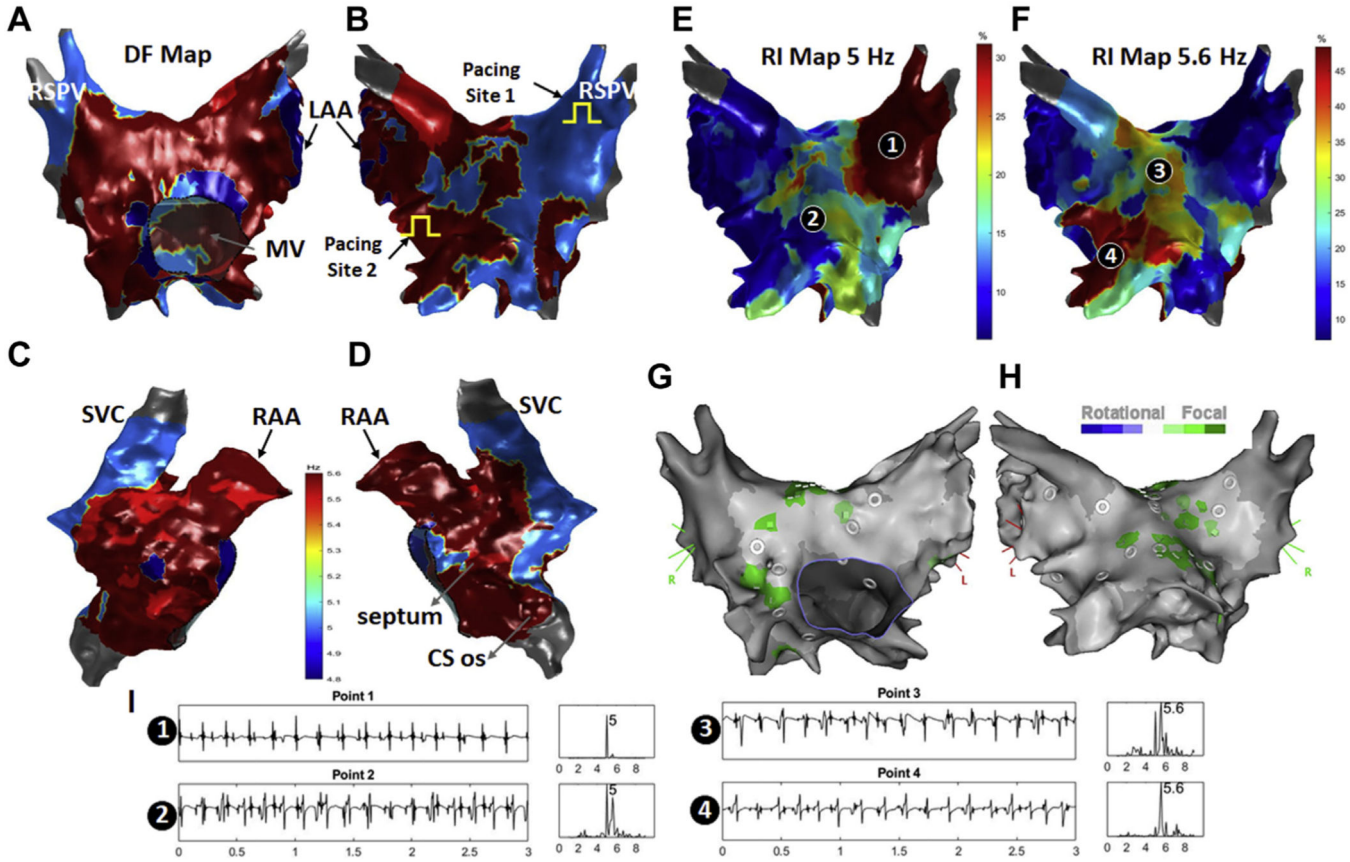

FIGURE 5. Fibrillatory Conduction During Dual-Site, Dual-Cycle Length Pacing From the RSPV at 200 ms (5 Hz) and Distal CS at 180 ms (5.6 Hz)

Frequency maps showing the distribution of the slower (5 Hz, **blue**) and faster (5.6 Hz, **red**) frequencies in an anterior (**A**) and posterior (**B**) view of the LA and a lateral (**C**) and septal (**D**) view of the RA. (**E and F**) RI maps of the 2 pacing frequencies. The maximum RI of 5 Hz is located near the RSPV and 5.6 Hz near the distal CS, demonstrating a correct identification of the 2 pacing sites. Also note the power gradient along the LA posterior wall moving away from the pacing site. (**G and H**) Cartofinder maps showing spurious annotations of FoA in the LA (**green**), with failure to identify either pacing site as a FoA. (**I**) Time and frequency domains of the 4 points identified in **E and F**. Abbreviations as in Figures 1, 2, and 4.

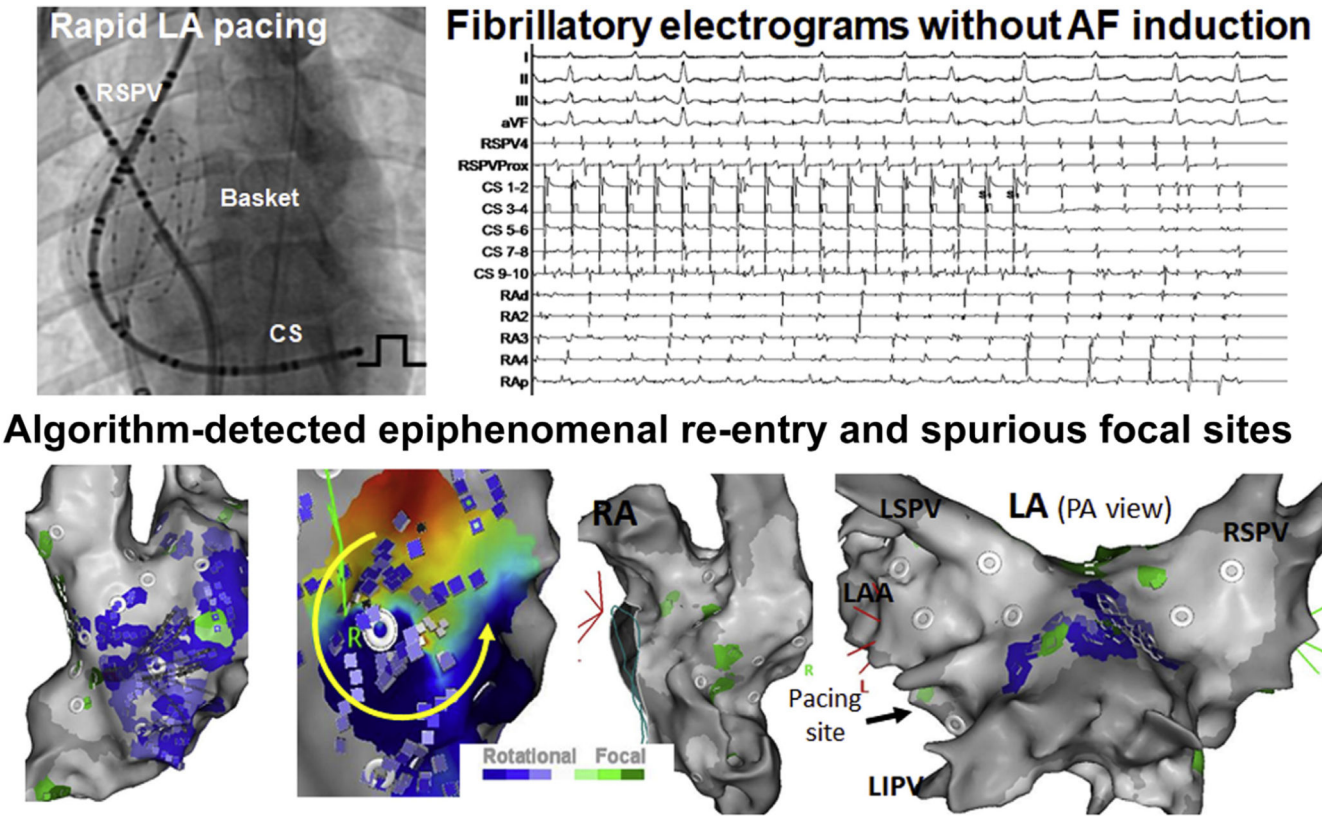

CENTRAL ILLUSTRATION. Epiphenomenal Re-Entry and Spurious Focal Activation During Rapid Pacing Without AF Induction

In an in vivo canine model, rapid left atrial (LA) pacing led to fibrillatory conduction with fibrillatory electrograms in the right atrium (RA) without atrial fibrillation (AF) induction (**top**). Cartofinder algorithm identified RoA most commonly in the RA, and spurious FoA sites away from the pacing site. The epiphenomenal nature of RoA in the absence of AF and the spurious FoA site identification question the value of mapping algorithms to guide ablation. CS = coronary sinus; FoA = focal activation; LIPV = left inferior pulmonary vein; RoA = rotational activations; RSPV = right superior pulmonary vein.

TABLE 1

A Summary of the Number of Maps in Each Atrium During Pacing and Induced AF Using the OctaRay

	Total Maps	With FoA (%)	With RoA (%)
RSPV pacing			
LA	98	59 (60)	–
RA	79	35 (44)	2(3)
Total	177	94 (53)	2(1)
CS pacing			
LA	83	66 (80)	3 (4)
RA	67	40 (59.7)	8 (11.9)
Total	150	106 (71)	11 (7)
Dual site pacing			
LA	98	54 (55)	3(3)
RA	54	31 (57)	4 (7)
Total	152	85 (56)	7(5)
Induced AF			
LA	105	72 (69)	2(2)
RA	95	72 (76)	8 (8)
Total	200	144 (72)	10 (5)

Values are n (%).

AF = atrial fibrillation; CS = coronary sinus; FoA = focal activations; LA = left atrium; RA = right atrium; RoA = rotational activations; RSPV = right superior pulmonary vein.